An Observing System Experiment with the West Coast Picket Fence

PAUL A. HIRSCHBERG

National Weather Service, Silver Spring, Maryland

PERRY C. SHAFRAN

National Centers for Environmental Prediction, Camp Springs, Maryland

RUSSELL L. ELSBERRY AND ELIZABETH A. RITCHIE

Naval Postgraduate School, Monterey, California

(Manuscript received 13 July 2000, in final form 8 February 2001)

ABSTRACT

Analyses and forecasts from a modern data assimilation and modeling system are used to evaluate the impact of a special rawinsonde dataset of 3-h soundings at seven sites interspersed with the seven regular sites along the West Coast (to form a so-called picket fence to intercept all transiting circulations) plus special 6-h rawinsondes over the National Weather Service Western Region. Whereas four intensive observing periods (IOPs) are available, only two representative IOPs (IOP-3 and IOP-4) are described here. The special observations collected during each 12-h cycle are analyzed with the National Centers for Environmental Prediction (NCEP) Eta Data Assimilation System in a cold start from the NCEP–National Center for Atmospheric Research reanalyses as the initial condition. Forecasts up to 48 h with and without the special picket fence observations are generated by the 32-km horizontal resolution Eta Model with 45 vertical levels.

The picket fence observations had little impact in some cases with smooth environmental flow. In other cases, relatively large initial increments were introduced offshore of the picket fence observations. However, these increments usually damped as they translated downstream. During IOP-3, the increments amplified east of the Rocky Mountains after only 24 h. Even though initially small, the increments in IOP-4 grew rapidly to 500-mb height increments ~20–25 m with accompanying meridional wind increments of 5–8 m s^{-1} that contributed to maxima in shear vorticity. Many of the downstream amplifying circulations had associated precipitation increments ~6 mm $(6\ h)^{-1}$ between the control and experimental forecasts. The equitable threat scores against the cooperative station set for the first 24-h forecasts during IOP-3 had higher values at the 0.50- and 0.75-in-thresholds for the picket fence dataset. However, the overall four-IOP equitable threat scores were similar.

Although the classical synoptic case was not achieved during the picket fence, these model forecasts suggest that such observations around the coast of the United States would impact the downstream forecasts when added in dynamically unstable regions. An ultimate picket fence of continuous remotely observing systems should be studied further.

1. Introduction

As numerical model predictions of midlatitude circulations have improved, the uneven quality and inhomogeneous space–time distribution of atmospheric observations is becoming the most significant factor hindering further improvements in the accuracy of weather forecasts (Emanuel et al. 1997). Although relatively high temporal resolution global satellite observations are increasingly being assimilated more effectively into numerical models (e.g., Caplan et al. 1997; Derber and Wu 1998), they have not yet completely offset forecast degradations owing to deficient in situ data (e.g., Kelly 1997; Tomassini et al. 1998). In particular, the relative lack of adequate observational data over upstream regions is often cited as a primary cause of 1–4-day forecast failures over regions in the United States (e.g., Emanuel et al. 1997; Langland et al. 1999).

To supplement satellite observations and pilot reports from commercial aircraft in observational data voids such as the world's oceans, observations from special aircraft reconnaissance are one possible option. For example, an instrumented aircraft that can release dropsondes may be deployed to intercept a disturbance of interest such as a tropical depression or an upper-level extratropical vorticity feature. This type of ''subjective'' targeting is based on the premise that acquiring mea-

Corresponding author address: Dr. Russell L. Elsberry, Department of Meteorology, Naval Postgraduate School, Code MR/Es, 589 Dyer Rd., Room 254, Monterey, CA 93943-5114.
E-mail: elsberry@nps.navy.mil

surements at the location of a disturbance will improve forecasts of the disturbance at some later time (Emanuel et al. 1997). While this approach has been demonstrated to have a positive impact on tropical cyclone track forecasts (e.g., Burpee et al. 1996), Emanuel et al. (1997) point out that it will work only if disturbance energy is advected in a very simple way. More sophisticated approaches may be necessary when disturbance energy propagates through the atmosphere at group velocities rather than local advection speeds, and when steering currents are changed by processes far from the disturbance of interest.

Recent predictability studies indicate that the impact of observations strongly depends on the observation locations or sampling strategy relative to so-called dynamically sensitive portions of the flow (e.g., Palmer et al. 1998). These studies support the notion that areas in which the initial condition error is likely to be both large and rapidly growing are the preferred areas to obtain supplementary observations (Emanuel et al. 1997). Over the last few years, several ''objective'' or ''adaptive'' targeting strategies to identify these preferred areas have been proposed (e.g., Bishop and Toth 1999; Buizza and Montani 1999; Pu et al. 1997; Gelaro et al. 1999). Field tests with aircraft dropsonde missions have included the Fronts and Atlantic Storm-Track Experiment (FASTEX; see Joly et al. 1999), North Pacific Experiment (Langland et al. 1999), California Land-falling Jets Experiment (Ralph et al. 1999), and the 1999 Winter Storm Reconnaissance Program (Szunyogh et al. 2000). Observation sensitivity results by including the special data from the Pacific-based adaptive observation field experiments have demonstrated 10% reductions in 2-day numerical model forecast error over operational control runs for the western United States verification region (Langland et al. 1999; Szunyogh et al. 2000).

Another potential observational sampling strategy to improve weather prediction within the interior of the United States is to increase the in situ observational network along or just outside the U.S. borders (Hirschberg et al. 1995). This so-called picket fence strategy to intercept and observe accurately features as they cross the coast may be justified based on studies with limited-area numerical models (e.g., Vukicevic and Errico 1990), which indicate that an accurate lateral boundary condition specification can enhance the predictability of synoptic- and mesoscale flows in the interior of the model domain. Given an appropriate horizontal spacing between stations, the picket fence measurements would monitor boundary fluxes of energy, mass, momentum, humidity, etc. In addition to providing continuous information about the boundary flow, the picket fence would accurately observe dynamically sensitive areas as they passed by.

To examine this picket fence concept, the spatial and temporal resolution of the National Weather Service (NWS) and Canadian Atmospheric Environmental Service (AES) operational rawinsonde network along the U.S. west coast was increased during the Stormscale Operational and Research Meteorology-Fronts Experiment Systems Test (STORM-FEST; Cunning and Williams 1993). The resulting picket fence (Fig. 1) consisted of seven special rawinsonde stations interspersed among the seven regular rawinsonde sites from Port Hardy, British Columbia, to San Diego, California. The picket fence stations recorded upper-air data from 3-h soundings during four intensive observing periods (IOPs) during February and March 1992 (see Hirschberg et al. 1995).

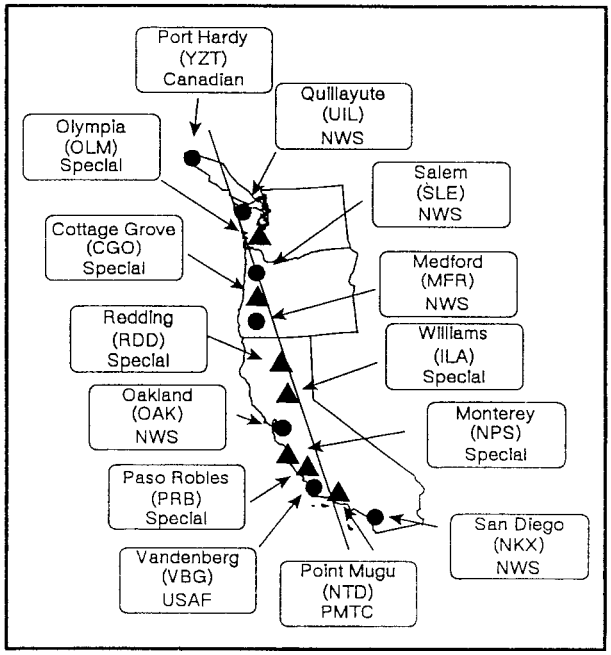

FIG. 1. Locations of the West Coast picket fence rawindsonde sites (NWS and AES sites, circles; special picket fence sites, triangles).

The specific objectives of the picket fence field experiment were to demonstrate (i) the operational feasibility of obtaining enhanced spatial and temporal observations via a quasi-linear array of extra observing stations; (ii) that the extra observations better resolved the space–time characteristics of the mass, heat, momentum, potential energy, kinetic energy, and moisture entering the United States from the Pacific Ocean; and (iii) that these extra observations improved downstream forecast accuracy. The field portion of the picket fence experiment demonstrated the operational feasibility of obtaining extra spatial and temporal observations via the picket fence approach, and is detailed in Lind et al. (1992).

The potential boundary condition impact of the picket fence was investigated in Hirschberg et al. (1995) by comparing the fluxes of mass, heat, momentum, potential energy, kinetic energy, and moisture across the West Coast resolved with various spatial and temporal combinations of picket fence data against a control calculation with only the 12-h regular upper-air sites. In par-

ticular, the flux quantities resolved by all picket fence stations at 3-h intervals were contrasted with those resolved by only the 12-h NWS and AES stations during two IOPs that represented systems that crossed the interior and periphery of the picket fence network, respectively. Hirschberg et al. (1995) demonstrated that new flux information is obtained from the extra picket fence spatial and temporal observations if the main synoptic feature crossed the middle of the enhanced observation network. In the best case (IOP-3) in which a wave system crossed the middle of the picket fence, significantly different fluxes were calculated with the full spatial and 3-h picket fence observations. Since the structure and location of the main circulation features were better defined, and the 3-h soundings provided increased temporal resolution, high-frequency variations in the fluxes accompanying the passage of the system were resolved that were not detected by the 12-h NWS-only calculations. In a more extensive IOP-4 case in which the main circulation center crossed the coast near the southern periphery of the enhanced observational network, little difference was detected between the enhanced picket fence and NWS-only analyses. In such cases, Hirschberg et al. (1995) hypothesize that NWS-only soundings adequately resolve the atmospheric circulations and boundary fluxes across the U.S. west coast because no significant mesoscale features were present for the special stations to detect.

The set of boundary flux calculations by Hirschberg et al. (1995) with and without the special picket fence data does not necessarily demonstrate that the extra picket fence observations have a downstream forecast impact. Clearly, the quantitative influence of the added observations on analysis and forecasting downstream needs to be documented. In the current study, analyses and forecasts with a modern four-dimensional data assimilation and modeling system are used to compare the impact of the special picket fence data relative to the current 12-h sounding network to determine whether better-resolved boundary fluxes indeed lead to significant forecast improvements.

2. Methodology

a. Eta Model

The model used in the picket fence experiments is the National Centers for Environmental Prediction (NCEP) mesoscale Eta Model (Black 1994). The eta coordinate is a step-mountain coordinate (Mesinger 1984), and the eta surfaces are nearly horizontal. The eta vertical coordinate is also normalized with respect to mean sea level pressure rather than surface pressure as in the sigma coordinate. A vertical Lorenz grid is used with 45 levels between the 20-m surface layer and the model top at 25 mb. The horizontal grid is an Arakawa E grid with 32-km spacing. The lateral boundary conditions are supplied by the NCEP–National Center for Atmospheric Research (NCAR) global reanalysis project (Kalnay et al. 1996). Deep and shallow convection are predicted with the Betts–Miller–Janjic scheme (Betts 1986; Betts and Miller 1986; Janjic 1994). Predictions of cloud water and ice are included (Zhao et al. 1997), and large-scale precipitation is produced from parameterized microphysics. Predicted clouds are included in the Geophysical Fluid Dynamics Laboratory radiation scheme (Fels and Schwartzkopf 1975; Lacis and Hansen 1974). The planetary boundary layer parameterization is a Mellor and Yamada (1982) level 2.5 model. The surface layer uses similarity functions from a Mellor–Yamada level 2.0 model. Finally, a coupled atmosphere–land surface package predicts the surface heat and moisture fluxes, as well as soil temperature and moisture, snow, and runoff. The package uses a multilayer soil model as well as vegetation and land-use fields that are the same as those used in the reanalysis. Snow depth analyses are obtained from the National Climatic Data Center archives.

Initial conditions at either 0000 or 1200 UTC for each control and experiment are created via a ''cold start'' procedure using the four dimensional Eta Data Assimilation System (EDAS); (Rogers et al. 1995) with observations during the previous 12-h period. The fields from the global reanalysis serve as the first initial guess for the EDAS at model start time minus 12 h. The assimilation uses all of the data types available in a standard NCEP dataset, including all of the 12-hourly rawinsonde soundings, surface land and marine data, profilers, aircraft reports, and satellites in the control and in addition to these, special picket fence and offtime 6-hourly NWS soundings in the experiment. These data are analyzed using a three-dimensional variational data assimilation (3DVAR) technique developed for the NCEP global system by Derber et al. (1991) and Derber and Parrish (1994) and extended to Eta applications by Parrish et al. (1996). Four analysis–forecast cycles are then made in which a 3-h forecast is generated that serves as the first guess for the next analysis, which includes available picket fence observations and offtime NWS soundings. Thus, each 12-h period during a picket fence IOP is treated as a separate data assimilation cycle to demonstrate the impact the special observations had on the Eta Model forecast from those initial conditions.

b. Experimental design

Four IOPs (Table 1) were available to study the effects of adding the special picket fence rawinsondes along the United States west coast. Most of the interpretations below will be based on the increments, which are defined as the experiment forecast initiated from an analysis that includes all picket fence special observations during the previous 12 h minus the control forecast. An alternate approach of comparing with the operational analyses at verifying times would not demonstrate as clearly the impact of the picket fence rawinsondes, since

TABLE 1. Experimental design for the picket fence comparison of the control experiment with the experiment using the special picket fence rawinsondes.

IOP	No. of cycles	First cycle	Last cycle	Times of picket fence files
1	2	1200 UTC 13 Feb	0000 UTC 14 Feb	0600 UTC 13 Feb–1800 UTC 13 Feb
2	4	0000 UTC 15 Feb	1200 UTC 16 Feb	1800 UTC 14 Feb–2100 UTC 16 Feb
3	3	0000 UTC 20 Feb	0000 UTC 21 Feb	0000 UTC 20 Feb–0000 UTC 21 Feb
4	5	1200 UTC 5 Mar	1200 UTC 7 Mar	0900 UTC 5 Mar–1200 UTC 7 Mar

this impact is generally smaller than the departures of both control and experimental forecasts from the analyses. Except in the STORM-FEST region over the central United States, the rawinsonde coverage is not adequate to resolve the specific locations and amplitudes of the changes introduced by the picket fence observations.

Each IOP consists of two to five individual cycles in which the 12-h EDAS is performed, and then a 48-h free forecast ensues from either 0000 or 1200 UTC.

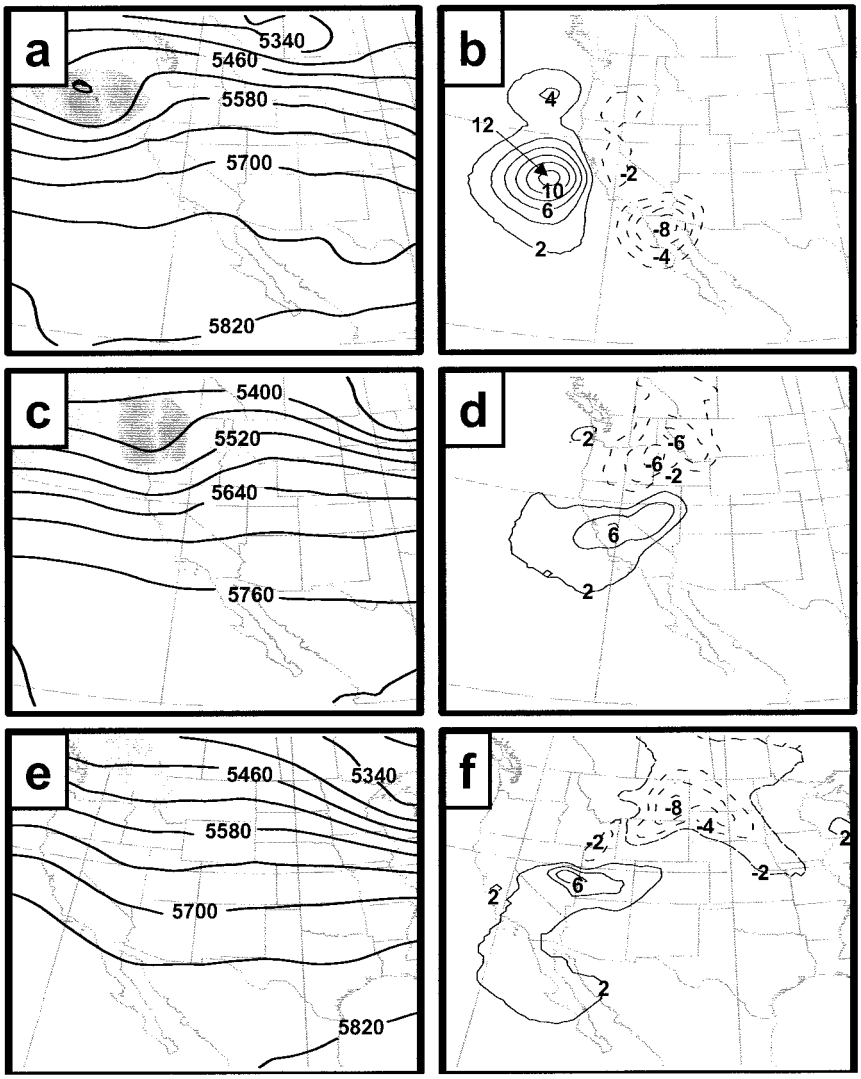

FIG. 2. Analyses of 500-mb height (m, solid) and sea level pressure (contours below 1008 mb shaded with 4-mb increments) during IOP-3 at (a) 0000 UTC 20 Feb, (c) 1200 UTC 20 Feb, and (e) 0000 UTC 21 Feb 1992. Increments (m, 2-m contour, solid positive, dashed negative) of 500-mb heights defined as the experiment–control forecast differences in (b), (d), and (f) that correspond to the times in (a), (c), and (e), respectively.

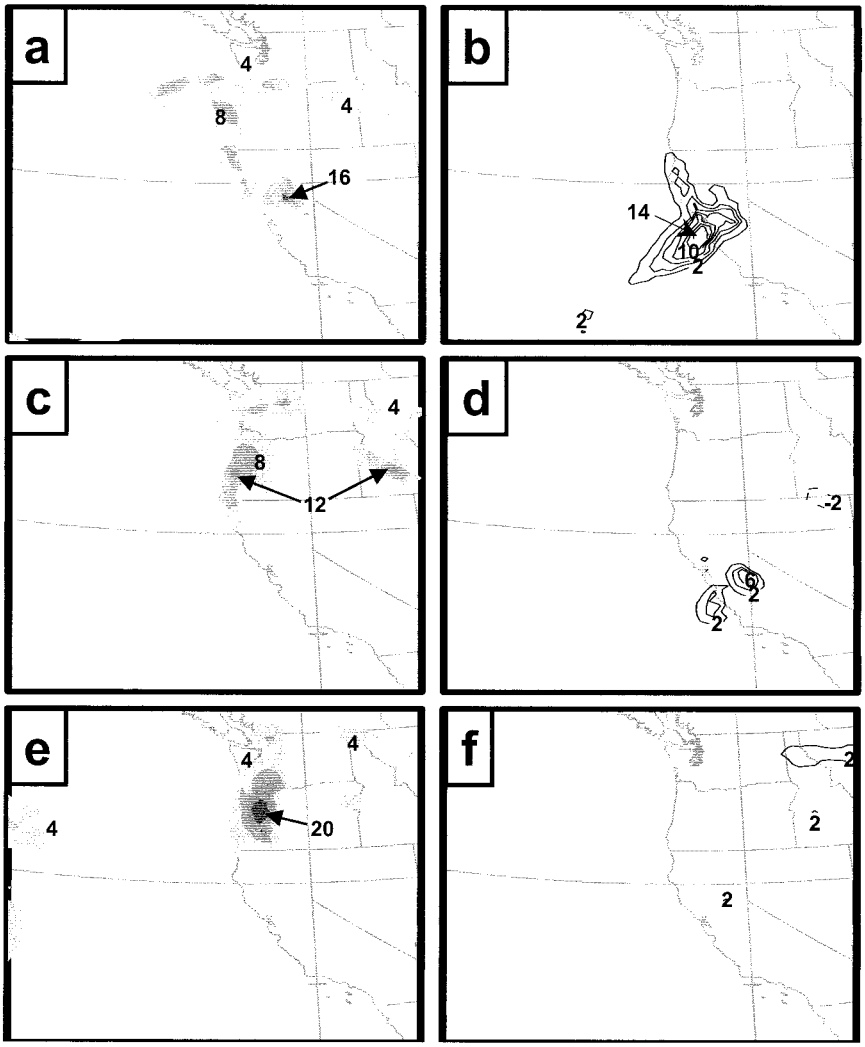

FIG. 3. Precipitation [mm (6 h)$^{-1}$ with contour increment of 4 mm (6 h)$^{-1}$, with shading beginning at 4 mm (6 h)$^{-1}$] during the prior 6 h predicted by the control Eta forecast at (a) 0600 UTC 20 Feb, (c) 1200 UTC 20 Feb, and (e) 1800 UTC 20 Feb 1992. Increments [mm (6 h)$^{-1}$ with 2 mm (6 h)$^{-1}$ intervals, dashed negative] of precipitation defined as the experiment–control forecast differences in (b), (d), and (f) corresponding to the times in (a), (c), and (e) respectively.

Only three selected cycles will be described here. Two of the cycles are the first and third during IOP-3, which is the IOP for which Hirschberg et al. (1995) found the largest differences in the boundary fluxes from the addition of the special picket fence observations. The third cycle is from IOP-4, for which the boundary fluxes were small, but in which the most active weather developed downstream over the STORM-FEST domain.

3. Intensive Observing Period-3

a. First cycle (0000 UTC 20 Feb 1992)

The synoptic situation in this first cycle is illustrated in Fig. 2a. A 500-mb short-wave trough is approaching the northern picket fence sites. However, the short wave is predicted in the control forecast to move across the Northwest and decrease in amplitude during the next 24 h (Figs. 2c and 2e). For this case, special picket fence observations were only available at the initial time of the model run (0000 UTC 20 Feb 1992). Nevertheless, the positive 500-mb increments from the inclusion of these observations indicates a weaker trough off most of the West Coast, with a slightly weaker ridge to the east (Fig. 2b). Already by 12 h into the forecast (Fig. 2d), the positive increments off the West Coast have moved onshore with the associated trough, but the magnitude has decreased to only 6 m. The experimental forecast has a weaker (6 m) ridge over Idaho after 12 h. By 24 h (Fig. 2f), this negative increment has rapidly propagated downstream, and amplified slightly, with a

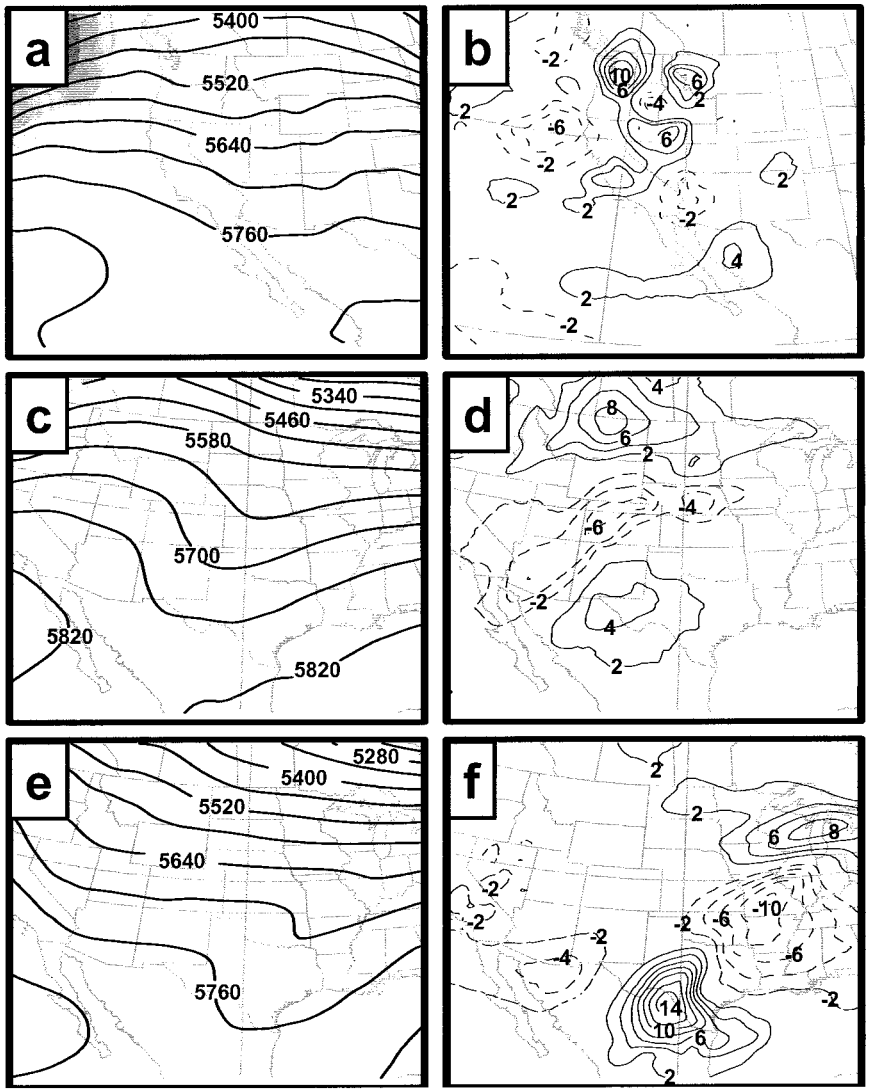

FIG. 4. Analyses and increments of 500-mb heights as in Fig. 2 except for later in IOP-3 at (a) 0000 UTC 21 Feb, (c) 0000 UTC 22 Feb, and (e) 0000 UTC 23 Feb 1992.

lobe of negative increments extending to the southeast. Comparison with the predicted field (Fig. 2e) indicates an apparent downstream propagation that is greater than the advective speed of the damping short-wave trough. The initial positive increment to the south has continued to move with the short-wave trough, but has not amplified or spread horizontally.

One positive impact of the picket fence observations was expected to be improved precipitation forecasts from the high spatial and temporal resolution moisture observations. The control forecast 6-h precipitation amounts ending at 6, 12, and 18 h (Figs. 3a, 3c, and 3e) suggest that precipitation continued throughout the 18 h along the Oregon and Washington coastal range. An east–west, and later a north–south, band of precipitation developed inland. The experimental forecast differences are 2 mm $(6\ h)^{-1}$ or less during the first 6 h for the Northwest coastal area (Fig. 3b), and only small regions with 2-mm differences are found with the inland precipitation maxima at 12 and 18 h (Figs. 3d and 3f). The largest precipitation differences in the experimental forecast are along the California coast, with a 14 mm $(6\ h)^{-1}$ increment in the first 6 h (Fig. 3b). This additional precipitation in the experimental prediction is between the positive and negative 500-mb height increments in Fig. 2a and is an example of how the picket fence observations can lead to short-term forecast differences. However, only small precipitation increments exist after 12 and 18 h (Figs. 3d and 3f).

In summary, the picket fence observations in the first 12-h cycle of IOP-3 did introduce changes in the initial fields. However, the short-wave system dampened inland, and little impact on the 500-mb height or precipitation forecasts could be found after 24 h. One inter-

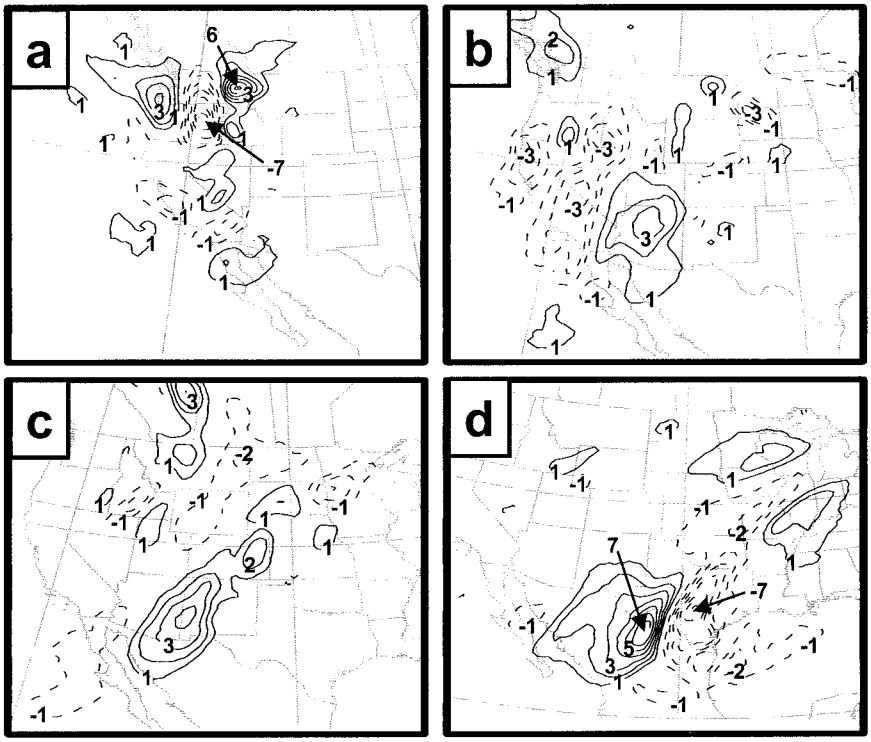

FIG. 5. Meridional wind increments (m s^{-1}, 1 m s^{-1} interval, dashed negative) at 500 mb defined as experiment–control during IOP-3 at (a) initial time of 0000 UTC 21 Feb and Eta forecasts after (b) 12, (c) 24, and (d) 48 h. Panel (c) corresponds to (c) and (d) in Fig. 4, and panel (d) corresponds to (e) and (f) in Fig. 4.

pretation for this lack of amplification of the increments based on the FASTEX field experiment (Langland et al. 1999; Gelaro et al. 1999; Szunyogh et al. 1999) is that the special observations were not in the regions of dynamic instability that lead to growth. The internal diffusion in the Eta Model will also contribute to a damping.

b. Third cycle (0000 UTC 21 Feb 1992)

Just 24 h later, a weak 500-mb trough over the northwest United States (Fig. 4a) is predicted in the control forecast to amplify by 24 h (Fig. 4c) and then move downstream in the westerly flow by 48 h (Fig. 4e). At the initial time, the impact of the special data is for generally small positive height increments over the Northwest, with small negative increments off the Oregon coast and over the California–Arizona border (Fig. 4b). Those positive and negative increment areas introduced by both the picket fence and 6-hourly NWS Western Region rawinsondes coalesce and slightly amplify by 24 h (Fig. 4d), with positive increments over Montana and western Texas bracketing an elongated negative increment from Arizona to Nebraska. This triple increment pattern continues at 48 h, with the northern positive increment propagating rapidly to the Great Lakes region. Both the central negative increment and the southern positive increment amplify during the 24-h period, with a +14 m increment over northeast Mexico.

The corresponding 500-mb meridional wind component increments are illustrated in Fig. 5. Although large (−7, +6 m s^{-1}) wind increments are introduced over the Northwest at the initial time (Fig. 5a), these very small spatial scale features do not persist for even 12 h (Fig. 5b). However, some elongated ±3 m s^{-1} increments are evident at 12 h (Fig. 5b) and the positive increment region has become more coherent by 24 h (Fig. 5c). A remarkable amplification then occurs over Texas at 48 h (Fig. 5d) as a −7 m s^{-1} (larger northerly) increment is ahead of a +7 m s^{-1} increment. This implied shear vorticity increment in the experimental forecast indicates a phase shift consistent with the 500-mb height increments in Fig. 4f.

The major band of 6-h precipitation associated with the trough approaching the Northwest during the first 6 h of the control forecast (Fig. 6a) is accompanied by precipitation increments of up to 6 mm (Fig. 6b). In this case, the experimental forecast brings the rain ashore a little earlier (later) in the northern (southern) band. During the next 36 h (Fig. 6c), the precipitation band moves slowly inland and decays. Only small [2 mm (6 h)$^{-1}$] increments are found in the 6-h precipitation prior to 36 h (Fig. 6d). By 48 h (Fig. 6e), a significant band of

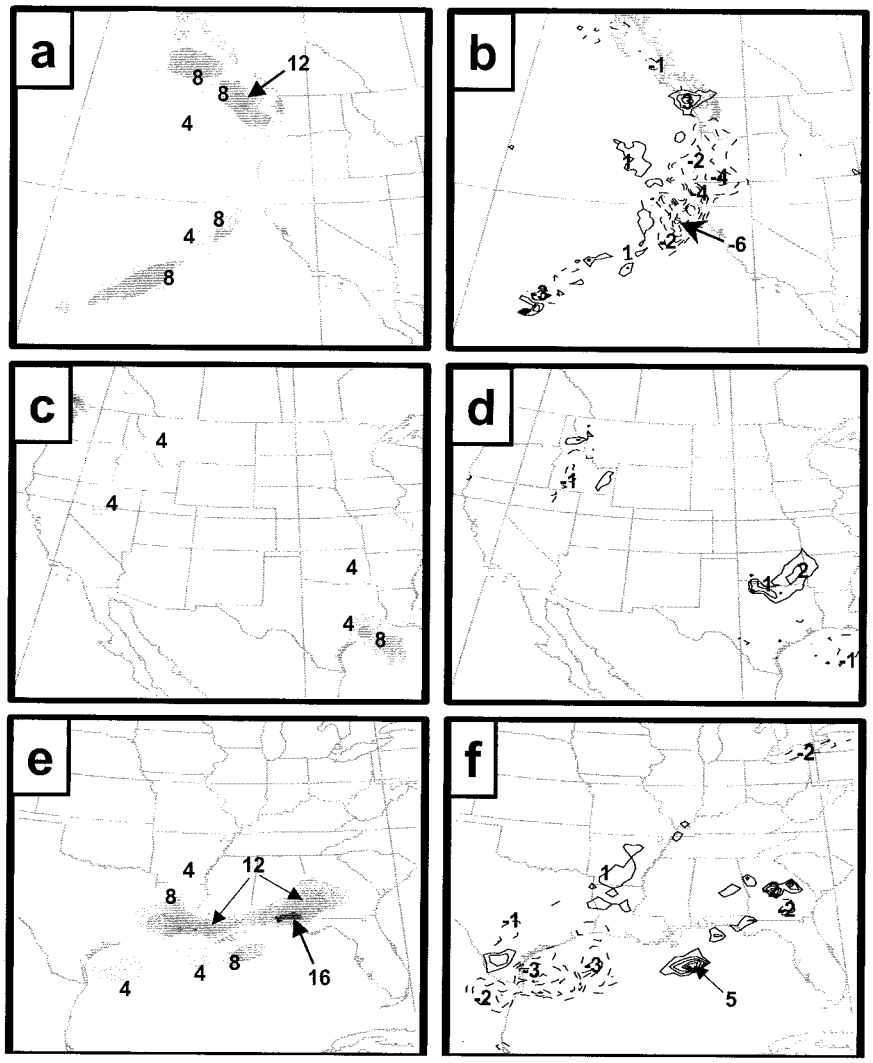

FIG. 6. Precipitation [mm (6 h)$^{-1}$] in the control and the corresponding increments [mm (6 h)$^{-1}$ contours] as in Fig. 3 except for IOP-3 forecasts beginning at 0000 UTC 21 Feb and verifying after (a) 6, (c) 36, and (e) 48 h.

precipitation is developing along the Gulf of Mexico coast in the control forecast. Although the differences near the Texas coast at 48 h (Fig. 6f) are only 3 mm (6 h)$^{-1}$ it appears that the 500-mb height (Fig. 4f) and meridional wind (Fig. 5d) increments from the picket fence observations are associated with these precipitation increments.

Verification of the precipitation forecasts is against the 24-hourly accumulations taken from the supplementary cooperative stations across the country, which are then analyzed to the model grid. Equitable threat scores (ETSs) are calculated from

$$\mathrm{ETS} = \frac{(C - E)}{(F + O - C - E)},$$

where C represents the number of grid points at which both the observation and the model value fall above a certain threshold (say, 0.5 in.), O is the number of observed points that fall above that threshold, F is the number of forecast points above the threshold, and $E = FO/T$, where T is the total number of points in the domain. A higher value of an ETS represents a better verification against observed precipitation.

The ETSs and bias scores for various precipitation thresholds during the first 24 h of all three cycles of IOP-3 are given in Figs. 7a and 7b. No significant ETS differences between the control and experimental forecasts are found for the 0.01-in, 0.10-in, and 0.25-in threshold verifications, and both forecasts have a large overprediction bias for these smaller amounts. A slight ETS improvement for the experimental forecast (Fig. 7a) is found for the 0.50-in. threshold and a rather large

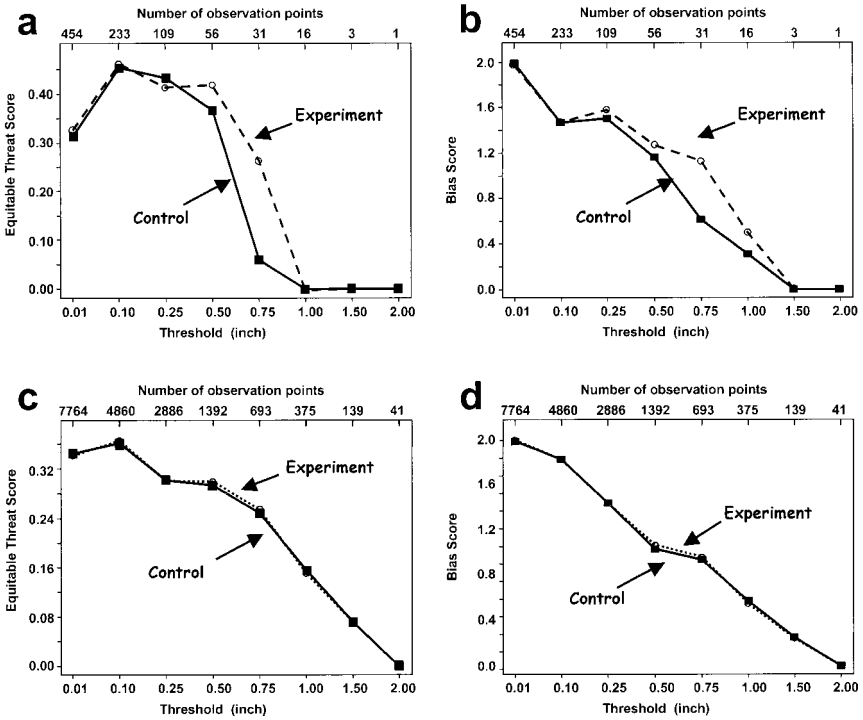

FIG. 7. (a) Equitable threat scores and (b) bias scores relative to the cooperative stations over the United States for various 24-h precipitation accumulation (in.) thresholds for the control (solid) and experimental (dashed) Eta forecasts during three cycles of IOP-3; (c) and (d) all cycles during all IOPs. The number of observation points for each threshold is indicated along the top.

ETS improvement is found for the 0.75-in. threshold. This improvement is not due to an overprediction as the bias scores (Fig. 7b) are close to 1.0 for these two thresholds. Only 16, 3, and 1 reports exceeded the 1.0-, 1.5-, and 2.0-in. thresholds, respectively, and neither model forecast was successful in delineating these larger precipitation areas (Fig. 7a), and both forecasts have a large underprediction bias (Fig. 7b) for these amounts. During IOP-3 the only precipitation reports over the cooperative station network were in the Northwest, so this summary with higher ETS scores for the 0.50- and 0.75-in thresholds is considered to be a favorable result.

By contrast, the first 24-h ETSs for all precipitation thresholds accumulated over the thousands of reports during all four IOP cycles during the picket fence period (Fig. 7c) are not significantly different for the control and the experimental forecasts. A similar bias pattern with over- (under-) prediction of small (large) amounts applies to both models for the all-IOP summary (Fig. 7d). This null ETS result might be expected since the ETS is calculated over the entire continental U.S. cooperative station network and precipitation is not occurring just in the Northwest or western U.S. areas. Additional observations from the seven picket fence rawinsondes and 6-h NWS Western Region rawinsondes would not be expected to affect the first 24-h forecast precipitation amounts at the central and eastern U.S. cooperative sites. Modifying the ETS/bias precipitation software to verify a positive regional impact with selected cooperative station reports is considered to be beyond the scope of this research effort.

4. Intensive Observing Period-4

Although IOP-4 had the most dramatic synoptic system during the picket fence experiment (Fig. 8), the amplitude of the offshore trough was so large that most of the energy flux crossed the West Coast south of the picket fence sites (Hirschberg et al. 1995). At least at 500 mb, the northern stations in the picket fence had offshore flow at 1200 UTC 7 March 1992 and only the southernmost sites had onshore flow that was fairly weak as the center was over the central California coast (Fig. 8a). By 24 (Fig. 8c) and 48 h (Fig. 8e), the control forecast slowly moved the deep trough northeastward to the Four Corners area. Notice the development of a sea level pressure trough (shading each 4 mb) east of the Rockies from Colorado southward into Mexico at 48 h (Fig. 8e).

The effect on the initial 500-mb heights from the special picket fence observations during the previous 12 h is a filling by 14 m (and weakening by 8 m) of

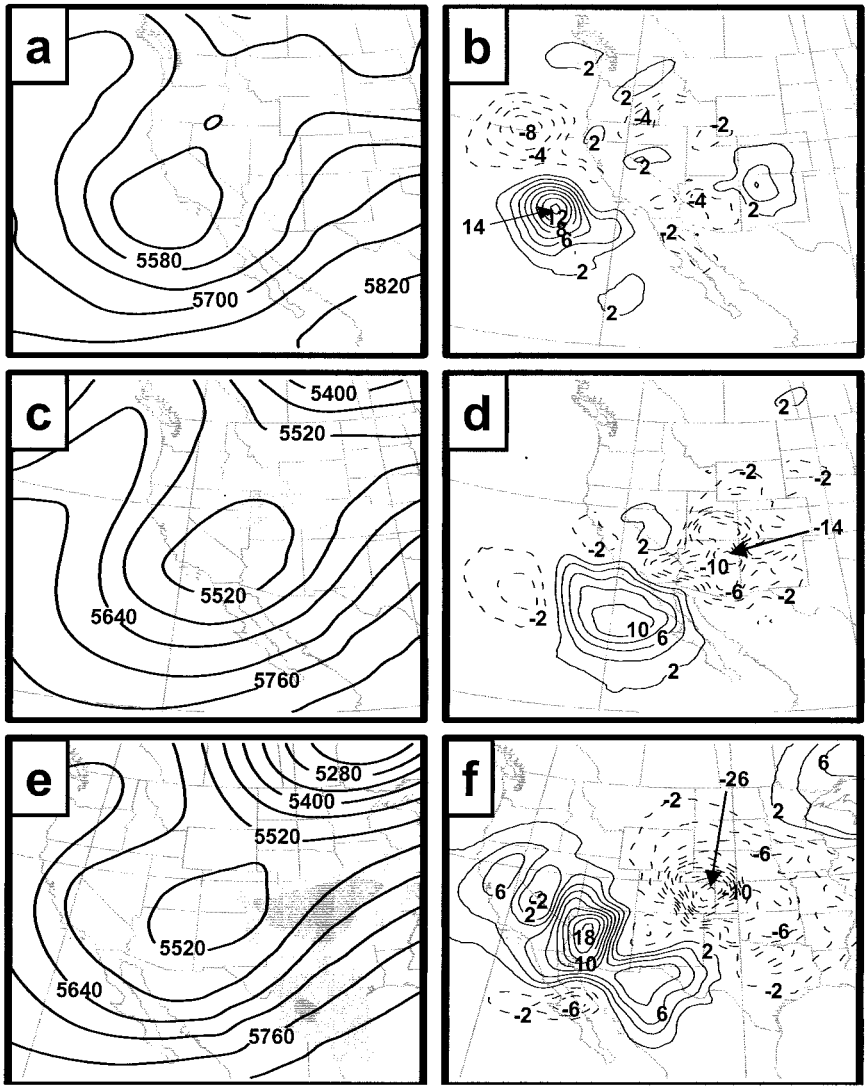

FIG. 8. Analyses and increments of 500-mb heights and sea level pressures as in Fig. 2 except for IOP-4 at (a) 1200 UTC 7 Mar, (c) 1200 UTC 8 Mar, and (e) 1200 UTC 9 Mar 1992.

the trough (ridge) to the west of southern (northern) California. Over the western United States, small increments in magnitude and horizontal scale are found at the initial time. By 24 h, the offshore area of positive increments has rotated cyclonically around the main trough to a position in northern Mexico, and has decreased in magnitude. The extensive area of negative height increments in Fig. 8d indicates the trough in the experimental forecast has advanced northeastward faster than in the control forecast. By 48 h (Fig. 8f), the area of positive increments has continued to rotate cyclonically into the region of the trough and has amplified to +18 m. More significantly, the negative anomaly has amplified from about −4 m at the initial time (Fig. 8b) to −14 m at 24 h (Fig. 8d) and to −26 m at 48 h (Fig. 8f). Especially during the 24–48-h period, the northeastward translation of the negative anomaly is faster than that of the trough–ridge system. Notice that this deeper 500-mb trough over Kansas in the experimental forecast is in the same region as the sea level pressure trough in Fig. 8e, which indicates that the low east of the Rocky Mountains is deeper.

The corresponding 500-mb meridional wind increments at 24 h (Fig. 9a) and 48 h (Fig. 9b) also indicate amplification in the region of negative 500-mb height increments (Fig. 8). Whereas the meridional wind increments at 24 h were about 5–6 m s^{-1}, two areas with positive–negative dipoles are found at 48 h near the deep 500-mb trough (Fig. 8e) and in conjunction with the negative height increment area over Kansas (Fig. 8f). Since the maximum (minimum) increments are +9 (−8) m s^{-1}, these dipoles represent significant differences in the shear of the meridional wind components between the control and experimental forecasts. Whether due to

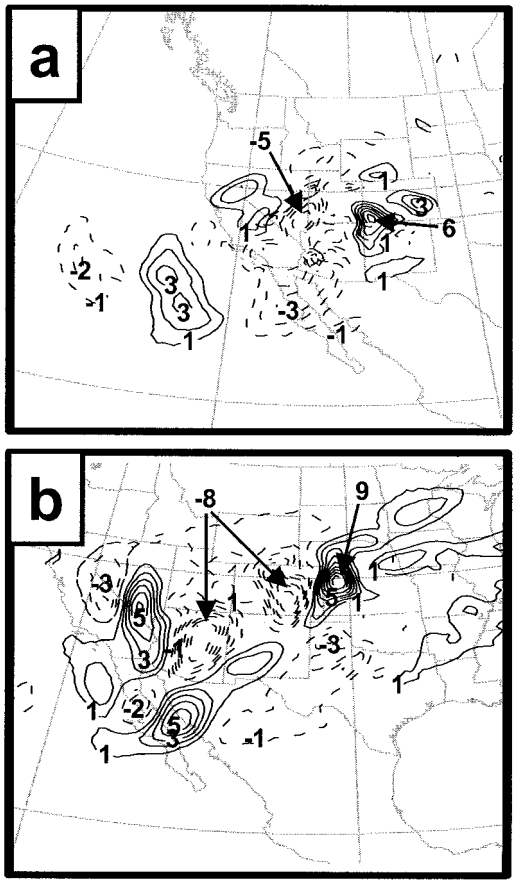

FIG. 9. Meridional wind increments as in Fig. 5 except for the (a) 24- and (b) 48-h forecasts from 1200 UTC 7 Mar during IOP-4. Panel (a) corresponds to (c) and (d) in Fig. 8, and panel (b) corresponds to (e) and (f) in Fig. 8.

phase or amplitude differences, the height and meridional wind increments that have developed between 24 and 48 h are noteworthy.

Although we do not have singular vectors as in the FASTEX analyses summarized by Gelaro et al. (1999), the amplification of the positive height increments and meridional wind dipole increments between 24 and 48 h is in an analogous ''dynamically sensitive'' area where growth of perturbations were found in FASTEX. Although a similar location relative to the upper-level jet and 500-mb trough does not guarantee the area is dynamically unstable, these conditions are consistent with forecaster experience. Because of the initial location of the negative height anomaly over the western United States, it is likely that the NWS Western Region rawinsondes were more important than the West Coast picket fence sondes in this case. It is noteworthy that significant growth can occur from quite small increments at the initial times, when those increments are in a dynamically unstable area (Palmer et al. 1998; Gelaro et al. 1999). Although similar or larger size increments were introduced by the picket fence observations in IOP-3 (Figs. 2b and 4b), these did not amplify significantly downstream, presumably because they were not in a dynamically unstable area (the short-wave trough damped).

In the control forecast at 12 h (Fig. 10a), only one small area of precipitation is predicted east of the trough. Both positive and negative precipitation increments of about 5 mm $(6\ h)^{-1}$ exist between the control and experimental forecasts (Fig. 10b), which are mainly associated with phasing differences. Both models then predict diminished and scattered precipitation over the western U.S. terrain through the next 24 h (Fig. 10c). In the 30–36-h period (Fig. 10c), a new small precipitation area along the Oklahoma–Texas border is predicted in both models, since the increment is at most about 1 mm $(6\ h)^{-1}$ (Fig. 10d). However, a major outbreak of precipitation occurs by 48 h (Fig. 10e) over Missouri with a trailing region of precipitation over Kansas and another narrow band extending southwestward into central Texas. Large areas with precipitation increments of about 4 mm $(6\ h)^{-1}$ (Fig. 10f) have developed between the two models from differences in the phases of the bands and the amplitude of the primary precipitation center. Whereas such differences may not be surprising in view of the height (Fig. 8f) and meridional wind increments (Fig. 9b), it is interesting that they arise from such small initial increments over the western United States. The suggested interpretation from the FASTEX results would be that such differences may be a result of small initial analysis differences in dynamically unstable regions.

The largest fractional change in any of the meteorological variables from the picket fence observations occurred in the relative humidity analyses. In the IOP-4 example above, the initial 500-mb relative humidity increments (Fig. 11a) include large areas of 50%. These differences arise in part because of the sensitivity of the univariate humidity analysis to gradients between the data-rich land areas and the data-sparse ocean areas, where the background field is the primary contributor. Baker and Daley (2000) illustrate a supersensitivity to the accuracy of any observations along such coastal regions, as the data assimilation system projects this information offshore into the data-sparse area. In general these large humidity increments tended to damp as they were advected with the flow. For example, the initial negative increment off the southern California coast is damped as it is rotated cyclonically around the deep trough by 12 h (Fig. 11b). Notice that the 36-h increments (Fig. 11c) are less than 10% over Oklahoma where the new area of precipitation was developing (Fig. 10c). However, the maximum 500-mb relative humidity increment at 48 h is again 50%. The close similarity in the increment patterns of humidity and precipitation (Fig. 10f) suggest that these midtropospheric humidity differences arise from vertical motion and moisture advection in association with the precipitation differences, rather than by downstream horizontal advection.

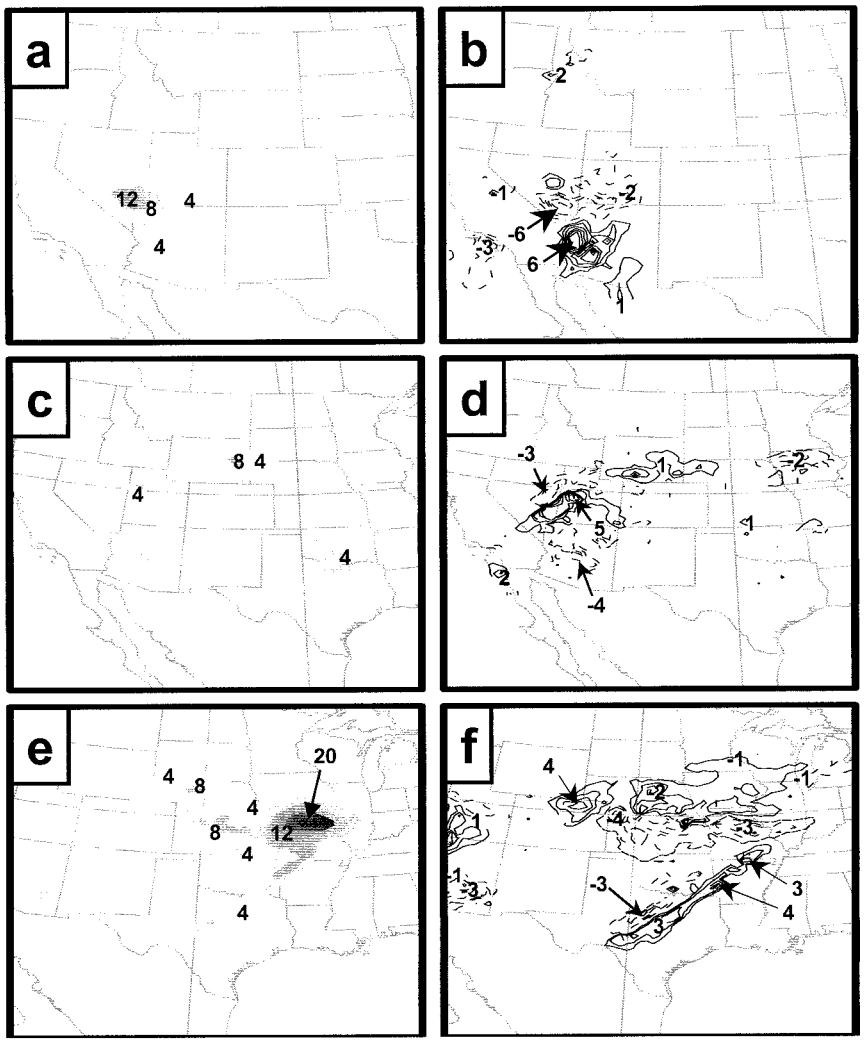

FIG. 10. Precipitation [mm (6 h)$^{-1}$] in the control and the corresponding increments [contours of mm (6 h)$^{-1}$] as in Fig. 3 except for IOP-4 forecasts beginning at 1200 UTC 7 Mar and verifying after (a) 12, (c) 36, and (e) 48 h.

5. Summary and discussion

The picket fence experiment was a logistical success in that 3-h rawinsonde soundings were collected at seven sites interspersed with the regular sites along the West Coast between Port Hardy and San Diego. Four IOPs of varying lengths in time were achieved through the cooperation of a number of agencies and volunteers (see description in Lind et al. 1992). These data provided higher spatial and temporal resolution in estimates of the fluxes across a line paralleling the picket fence sites (Hirschberg et al. 1995). In some situations with smaller-scale features present, the boundary fluxes including the picket fence observations were larger than from the regular rawinsonde sites with 12-h resolution. However, it remained to be demonstrated that these differences in ''upstream boundary conditions'' would have a substantial effect on numerical weather predictions over the United States, and specifically over the target STORM-FEST area with enhanced meteorological observations.

The West Coast picket fence soundings within a 12-h window (plus special 6-h rawinsondes over the NWS Western Region) were analyzed with the Eta Data Assimilation System, which is a regional 3DVAR system, and integrated to 48 h in a 32-km horizontal resolution Eta Model with 45 levels in the vertical. The primary fields analyzed here are the experiment–control increments, because the purpose is to illustrate that the addition of the special picket fence observations would change the Eta Model forecasts. Since none of the circulation systems verified over the STORM-FEST special rawinsondes, verification of the mesoscale features introduced by the picket fence observations is difficult as such amplitude and phase differences are not resolved well by the conventional network.

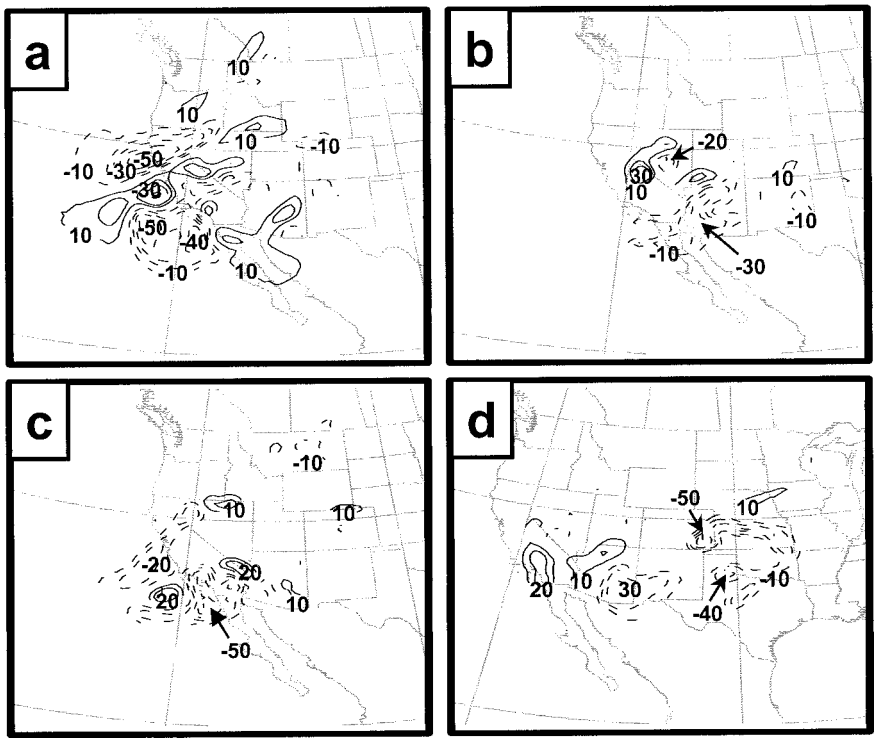

FIG. 11. Relative humidity (%) increments defined as experiment–control forecast differences during IOP-4 at (a) initial time 1200 UTC 7 Mar and forecasts after (b) 12, (c) 36, and (d) 48 h.

In many cases (including IOPs-1 and -2 and the early part of IOP-4 not discussed here), the interspersed rawinsondes had a limited effect. That is, the regular rawinsonde sites were often adequate to resolve the horizontal scales of the circulation crossing the picket fence. The analyses that included the picket fence observations occasionally did have sizeable increments, especially offshore and in the relative humidity fields. Offshore increments may be introduced by the horizontal structure functions in the objective analysis that extend data from the land areas to the offshore areas, where the analyses may also be affected by offshore advection represented in the background fields from the previous model integration. During the picket fence period, nearly all of the increments were advected downstream with the synoptic flow and generally damped after at most a brief amplification. This damping was particularly noted with the relative humidity increments. At other times, the increments rapidly propagated downstream at speeds greater than the translation with the synoptic circulation. Thus, increments introduced by the West Coast picket fence observations could at selected times be found over the Midwest by 48 h.

Late in IOPs-3 and -4, the increments introduced by the picket fence and extra NWS observations amplified east of the Rocky Mountains after 36–48 h. Examples were illustrated in which sizeable 500-mb height increments between the control and experimental forecasts were accompanied by meridional wind dipoles that have large shear vorticity values. The distinguishing feature between these amplifying and damping increments is interpreted to be that they have moved into a dynamically unstable area (e.g., in advance of a developing synoptic wave during IOP-4). That is, both phase differences and amplification appear to play a role in these amplification cases. Corresponding 6-h precipitation accumulation increments were documented in these amplifying perturbations. In general, the increments were modulations of features in the control forecast, rather than being completely unresolved weather events.

The ETS for the first 24-h precipitation during IOP-3 indicated a more skillful prediction for the thresholds of 0.50 and 0.75 in. when the picket fence observations were included. Since the corresponding bias scores are near 1.0 for these two thresholds, this favorable result is not simply due to overpredicted rainfall amounts. Even though the cooperative station observations in the ETS included the entire United States, this positive result is consistent with the only precipitation area during IOP-3 being in the western United States where the picket fence observations might indeed be expected to improve 24-h precipitation scores. When all 14 picket fence cycles were included, and precipitation was not just limited to the western United States, no significant difference in 24-h precipitation threat scores could be documented. A regional ETS verification system following only those precipitation systems affected by the

picket fence observations would be necessary to document an overall positive regional impact.

As is often the case in a short field experiment of opportunity, the anticipated ''classical'' case of an intense jet stream and/or vigorous short wave was not documented crossing the picket fence. Thus, the picket fence strategy of having a higher spatial and temporal resolution in such a case remains to be tested. Although a short wave was observed during IOP-3, it was a mature wave that damped quickly as it moved inland. Whereas a strong jet was present during IOP-4, it crossed the coast south of the picket fence.

Because of the different advective/propagation paths downstream from the West Coast, the objective of tracing a better-resolved feature directly to the STORM-FEST observing region was generally not achieved. Based on this limited sample, it may be difficult to anticipate a downstream area of impact without an adjoint sensitivity or ensemble transform technique that have recently been used in FASTEX and other targeted observation experiments (Langland et al. 1999). Such techniques are not available for the picket fence period.

A limitation of this assimilation is that each 12-h cycle was a ''cold start'' using the 12-h previous control forecast from the NCEP–NCAR reanalysis as background field and only the regular and special observations during that 12-h period. That is, a regional model update strategy of analysis–forecast–analysis was not used, because the desire was that the separate contribution from each 12-h cycle could be evaluated. A continuing regional model update cycle throughout the IOP would have propagated the accumulated effects of the picket fence observations farther downstream. However, it would have been more difficult to trace which 12-h cycle contributed to an improvement, as a specific downstream target may be impacted from multiple ray paths originating at different times.

An obvious conclusion is that a larger picket fence that includes more stations to the south and north is needed to capture subtropical jet events over the Baja Peninsula and trough passages over western Canada. The ultimate application of the picket fence strategy would be a permanent set of ground-based profiling instruments around the U.S. coasts and borders that would observe continuously, or on an ''as needed'' basis, the winds, temperature, humidity, etc. When synoptic conditions are relatively quiescent, NWS-only soundings may be adequate for analyzing the atmospheric conditions and defining the boundary fluxes across the west coast of the United States. It may be scientifically sound, besides being more cost effective, to make special or adaptive rawinsonde observations only on an intermittent as needed basis. For instance, portions of a future picket fence could be activated for flexible time periods based on some reasonable assessment of the timing and location of the West Coast passage of significant, dynamically sensitive portions of the flow that may trigger significant weather over the United States.

Acknowledgments. This research has been sponsored by the National Science Foundation. Special thanks go to the volunteer observers who collected these observations. Drs. Geoff DiMego and Eric Rogers of NCEP/EMC provided support and guidance in carrying out these comparisons. Mrs. Penny Jones skillfully prepared the manuscript.

REFERENCES

Baker, N. L., and R. Daley, 2000: Observation and background sensitivity in the adaptive observation-targeting problem. *Quart. J. Roy. Meteor. Soc.,* **126,** 1431–1454.

Betts, A. K., 1986: A new convective adjustment scheme. Part I: Observational and theoretical basis. *Quart. J. Roy. Meteor. Soc.,* **112,** 1306–1335.

——, and M. T. Miller, 1986: A new convective adjustment scheme. Part II: Single tests using GATE wave, BOMEX, and Arctic airmass data. *Quart. J. Roy. Meteor. Soc.,* **112,** 693–709.

Bishop, C., and Z. Toth, 1999: Ensemble transformation and adaptive observations. *J. Atmos. Sci.,* **56,** 1748–1765.

Black, T. L., 1994: The new NMC mesoscale Eta Model: Description and forecast examples. *Wea. Forecasting,* **9,** 265–278.

Buizza, R., and A. Montani, 1999: Targeted observations using singular vectors. *J. Atmos. Sci.,* **56,** 2965–2985.

Burpee, R. W., J. L. Franklin, S. J. Lord, R. E. Tuleya, and S. D. Aberson, 1996: The impact of omega dropwindsondes on operational hurricane track forecast models. *Bull. Amer. Meteor. Soc.,* **77,** 925–933.

Caplan, P., J. Derber, W. Gemmill, S. Y. Hong, H.-L. Pan, and D. Parrish, 1997: Changes to the 1995 NCEP operational medium-range forecast model analysis/forecast system. *Wea. Forecasting,* **12,** 581–594.

Cunning, J. B., and S. F. Williams, 1993: U.S. Weather Research Program STORM-FEST operations summary and data inventory. U.S. Weather Research Program Office, 389 pp.

Derber, J. C., D. F. Parrish, W.-S. Wu, Z. Pu, and S. R. H. Rizvi, 1994: Improvements to the operational SSI global analysis system. Preprints, *10th Conf. on Numerical Weather Prediction,* Portland, OR, Amer. Meteor. Soc., 149–150.

——, and W.-S. Wu, 1998: The use of TOVS cloud-cleared radiances in the NCEP SSI analysis system. *Mon. Wea. Rev.,* **126,** 2287–2299.

——, D. F. Parrish, and S. J. Lord, 1991: The new global operational analysis system at the National Meteorological Center. *Wea. Forecasting,* **6,** 538–547.

Emanuel, K., and Coauthors, 1997: Observations in aid of weather prediction for North America: Report of Prospectus Development Team Seven. *Bull. Amer. Meteor. Soc.,* **78,** 2859–2868.

Fels, S. B., and M. D. Schwartzkopf, 1975: The simplified exchange approximation: A new method for radiative transfer calculations. *J. Atmos. Sci.,* **32,** 1475–1488.

Gelaro, R., R. Langland, G. D. Rohaly, and T. E. Rosmond, 1999: An assessment of the singular vector approach to targeted observation using the FASTEX data set. *Quart. J. Roy. Meteor. Soc.,* **125,** 3299–3328.

Hirschberg, P. A., R. J. Lind, S. J. Bolduc, and R. L. Elsberry, 1995: The West Coast picket fence experiment during STORM-FEST. *Bull. Amer. Meteor. Soc.,* **76,** 1741–1757.

Janjic, Z. I., 1994: The step-mountain eta coordinate model: Further developments of the convection, viscous sublayer, and turbulence closure schemes. *Mon. Wea. Rev.,* **122,** 927–945.

Joly, A., and Coauthors, 1999: Overview of the field phase of the Fronts and Atlantic Storm-Track Experiment (FASTEX) project. *Quart. J. Roy. Meteor. Soc.,* **125,** 3131–3163.

Kalnay, E., and Coauthors, 1996: The NCEP/NCAR 40-Year Reanalysis Project. *Bull. Amer. Meteor. Soc.,* **77,** 437–471.

Kelly, G., 1997: Influence of observations on the operational ECMWF system. *WMO Bull.,* **46,** 336–341.

Lacis, A. A., and J. E. Hansen, 1974: A parameterization of the absorption of solar radiation in the earth's atmosphere. *J. Atmos. Sci.,* **31,** 118–131.

Langland, R. H., and Coauthors, 1999: The North Pacific Experiment (NORPEX-98): Targeted observations for improved North American weather forecasts. *Bull. Amer. Meteor. Soc.*, **80,** 1363–1384.

Lind, R. J., P. A. Hirschberg, D. W. Titley, and R. L. Elsberry, 1992: West Coast picket fence feasibility study during STORM-FEST. I. Field program summary. Naval Postgraduate School Tech. Rep. NPS-MR-92-003, 140 pp.

Mellor, G. L., and T. Yamada, 1982: Development of a turbulence closure model for geophysical fluid problems. *Rev. Geophys. Space Phys.,* **20,** 851–875.

Mesinger, F., 1984: A blocking technique for representation of mountains in atmospheric models. *Riv. Meteor. Aeronaut.,* **44,** 195–202.

Palmer, T. N., R. Gelaro, J. Barkmeijer, and R. Buizza, 1998: Singular vectors, metrics, and adaptive observations. *J. Atmos. Sci.,* **55,** 633–653.

Parrish, D., J. Purser, E. Rogers, and Y. Lin, 1996: The regional 3D-variational analysis for the Eta Model. Preprints, *11th Conf. on Numerical Weather Prediction,* Norfolk, VA, Amer. Meteor. Soc., 454–455.

Pu, Z.-X., E. Kalnay, J. Sela, and I. Szunyogh, 1997: Sensitivity of forecast error to initial conditions with a quasi-inverse linear method. *Mon. Wea. Rev.,* **125,** 2479–2503.

Ralph, F. M., and Coauthors, 1999: The California Land-Falling Jets Experiment (CALJET). Objectives and design of a coastal atmosphere ocean observing system deployed during a strong El Nino. Preprints, *Third Symp. on Integrated Observing Systems,* Dallas, TX, Amer. Meteor. Soc., 78–81.

Rogers, E., D. G. Deaven, and G. J. DiMego, 1995: The Regional Analysis System for the operational Eta Model: Original 80-km configuration, recent changes, and future plans. *Wea. Forecasting,* **10,** 810–825.

Szunyogh, I., Z. Toth, K. A. Emanuel, C. H. Bishop, C. Snyder, R. E. Morss, J. Wollen, and T. Marchok, 1999: Ensemble-base targeting experiments during FASTEX: The impact of dropsonde data from the Learjet. *Quart. J. Roy. Meteor. Soc.,* **125,** 3189–3218.

——, ——, R. E. Morss, S. J. Majumdar, B. J. Etherton, and C. Bishop, 2000: The effect of targeted dropsonde observations during the 1999 Winter Storm Reconnaissance Program. *Mon. Wea. Rev.,* **128,** 3520–3537.

Tomassini, M., G. Kelly, and R. Saunders, 1998: Use and impact of satellite atmospheric motion winds on ECMWF analyses and forecasts. *Mon. Wea. Rev.,* **127,** 971–986.

Vukicevic, T., and R. M. Errico, 1990: The influence of artificial and physical factors upon predictability estimates using a complex limited-area model. *Mon. Wea. Rev.,* **118,** 1460–1482.

Zhao, Q., T. L. Black, and M. E. Baldwin, 1997: Implementation of the cloud prediction scheme in the Eta Model at NCEP. *Wea. Forecasting,* **12,** 697–712.